

# Quality-based generation of weather radar Cartesian products

K. Ośródka and J. Szturc

Institute of Meteorology and Water Management – National Research Institute, PL-01-673  
Warszawa, ul. Podleśna 61, Poland

Correspondence to: jan.szturc@imgw.pl

## Abstract

Weather radar data volumes are commonly processed to obtain various 2D Cartesian products based on the transfer from polar to Cartesian representations through a certain interpolation method. In this research an algorithm of the spatial interpolation of polar reflectivity data employing *QI* (quality index) data is applied to find the Cartesian reflectivity as PPI (plan position indicator) products. On this basis, quality-based versions of standard algorithms for the generation of the following products have been developed: ETOP (echo top), MAX (maximum of reflectivity), and VIL (vertically integrated liquid water). Moreover, as an example of a higher-level product, a CONVECTION (detection of convection) has been defined as a specific combination of the above-listed standard products. A corresponding quality field is determined for each generated product, taking into account the quality of the pixels from which a given product was determined and how large a fraction of the investigated heights was scanned. Examples of such quality-based products are presented in the paper.

## 1 Introduction

Weather radar measurements of reflectivity are burdened with numerous errors that are caused by both technical and meteorological factors (e.g. review by Villarini and Krajewski, 2010). These errors are recognised thanks to intensive empirical work performed at the national level (by national meteorological services) and at the international level, e.g. in the frame of weather radar-related COST (European Cooperation in Science and Technology)

30 Actions (Michelson et al., 2005) or the BALTRAD (An Advanced Weather Radar Network  
31 for the Baltic Sea Region) project (Michelson et al., 2012).

32 The next step after error identification is the development of algorithms that can help to  
33 correct the data (Einfalt and Michaelides, 2008). Simultaneously to the correction of data, its  
34 quality can be estimated quantitatively, e.g. by means of quality index  $QI$  (Einfalt et al., 2010;  
35 Norman et al., 2010). Related research work, which has become more advanced with  
36 continuous progress in the field of correction algorithms, has continued with a view to  
37 operational work (Germann and Joss, 2004; Ośródką et al., 2010; Elo, 2012; Szturc et al.,  
38 2012a).

39 Raw weather radar data are generated as so called volumes, i.e. 3D polar data. Practically,  
40 such volumes consist of sets of measurement gates organised in polar scans related to the  
41 rotation of an antenna at selected elevation angles. Based on the transfer from polar to  
42 Cartesian representations through a certain interpolation method the volumes are processed to  
43 obtain various 2D Cartesian products dedicated to specific user requirements (Heistermann et  
44 al., 2013).

45 The transformation is not a trivial task because the distances between neighbouring polar  
46 gates considerably vary with their location in relation to the distance to the radar site and scan  
47 strategy. It was analysed how much information is lost during this transformation and it  
48 turned out that the effect of the conversion of polar to Cartesian coordinates is significant,  
49 especially for smaller catchments such as urban or mountainous ones (Gonzalez-Ramirez and  
50 Cluckie, 2006). Research works have been undertaken to improve the transformation,  
51 especially in terms of radar precipitation estimation. For instance, Henja and Michelson  
52 (1999) stated that employing some distance-weighting technique is more appropriate than  
53 using the value from the nearest gate. At present such techniques are operationally employed  
54 in different hydrological systems (e.g. Harrison et al., 2009; Elo, 2012).

55 The main assumption of the presented work is to ensure maximum reliability of the final  
56 products, so the transformation and subsequent specific product generation should be quality-  
57 based, i.e. particular algorithms should be designed taking into account the quality of  
58 particular measurement gates. Therefore the quality index fields assigned to reflectivity  
59 volumes should play an essential role in the task of 2D product generation.

60 The paper is organised as follows. Since information about the weather radar data quality  
61 (expressed as quality index  $QI$ ) is incorporated into radar product definitions in the research,

62 the method of quality characterisation is briefly described in Sect. 2.2. The technique of  
63 quality control is based on algorithms developed for the RADVOL-QC package (Sect. 2.3).  
64 Having 3D volumes of reflectivity and relevant quality information, the set of 2D Cartesian  
65 PPI (plan position indicator) products may be generated (Sect. 3.1) together with  
66 corresponding quality fields (Sect. 3.2). The quality-based PPIs constitute a starting point for  
67 the generation of more sophisticated products such as: echo top (ETOP), maximum of  
68 reflectivity (MAX) and vertically integrated liquid water (VIL) (Sect. 4.1). As well as this, a  
69 non-standard product named CONVECTION, which is dedicated to the identification of  
70 convective area based on all the previously described products, is defined. In Sect. 4.2, the  
71 technique of *QI* field determination for the above products is described. Validation of the  
72 quality-based products is described and discussed in Sect. 5, and finally their examples are  
73 demonstrated in Sect. 6.

74

## 75 **2 The characterisation of 3D weather radar data quality**

### 76 **2.1 Data**

77 The framework of quality-based products generation has been tested on data from the Polish  
78 weather radar network POLRAD operated by the Institute of Meteorology and Water  
79 Management – National Research Institute (IMGW-PIB), which is a national meteorological  
80 service in Poland. The network consists of eight C-Band radars with the scan strategy defined  
81 in Table 1. The strategy includes 10 scans at elevations from 0.5 to 23.8° with a beam width  
82 of 1°. Sampling is performed every kilometre along the beam of 360° in azimuths.

### 83 **2.2 Quality index approach**

84 The quantitative estimation of error magnitude is necessary not only in order to gain general  
85 knowledge about data uncertainty, but also to apply quality information in further data  
86 processing, e.g. in the generation of standard or user-related specific products. One of the  
87 most common approaches in the characterisation of the quality of weather radar data is to  
88 employ quality index (*QI*) that is defined as a unitless quantity which provides information on  
89 the data reliability in a digital scale. Most often, the *QI* ranges from 0 (for the poorest quality)  
90 to 1 (for the best data), according to EUMETNET OPERA (Operational Programme for the  
91 Exchange of Weather Radar Information) definition (Michelson et al., 2014), but other scales  
92 can also be applied (see review provided by Einfalt et al., 2010).

93 Each category of errors burdening radar data is characterised by specific properties, spatial  
94 and temporal structure, and the possibility of diagnosis and correction; this consequently  
95 requires dedicated quality control techniques. Thus, the processing of the radar data is  
96 performed in a certain number of steps and after each one the data quality improves and a  
97 particular *QI* field is generated. Having determined a set of quality indices, a total *QI* field  
98 describing overall data quality can be computed, most often by using a multiplicative scheme  
99 (e.g. Fornasiero et al., 2005; Germann et al., 2009; Ośródką et al., 2014).

## 100 **2.3 RADVOL-QC algorithms**

101 In this research the quality control of radar reflectivity volumes was performed by means of  
102 dedicated software RADVOL-QC, which was developed to correct the data and generate *QI*  
103 fields (Ośródką et al., 2014). The software was integrated with the BALTRAD system for  
104 radar data exchange (Michelson et al., 2012), where it can work on data in HDF5 file format  
105 according to the EUMETNET OPERA digital information model ODIM (OPERA Digital  
106 Information Model) (Michelson et al., 2014). Additionally, in the IMGW-PIB the RADVOL-  
107 QC version developed for Gematronik Rainbow radar software works operationally since  
108 2014 as a volume postprocessing of data in native Rainbow format.

109 The RADVOL-QC is a system designed for quality control of 3D volumes in polar  
110 coordinates, which includes the data corrections and *QI* determination due to each recognised  
111 error source, and aggregation of the particular *QIs* into total *QI* using multiplicative scheme.  
112 At present the system consists of the following algorithms (Ośródką et al., 2014; Szturc et al.,  
113 2012b):

- 114 – quality characterisation due to effects related to the distance to the radar site (BROAD),
- 115 – removal of conventional non-meteorological echoes (NMET),
- 116 – removal of geometrically-shaped non-meteorological echoes caused by external signal  
117 interference (SPIKE),
- 118 – removal of measurement noise (SPECK),
- 119 – correction due to partial and total beam blockage (BLOCK),
- 120 – correction due to attenuation in rain (ATT).

121 The algorithms enable both the correction of data (excepting BROAD) and the estimation of  
122 the quality of corrected data expressed as *QI*. It should be emphasized that if a specific gate is

123 found burdened with an error, its quality index is reduced even though the reflectivity value is  
124 improved, because each correction algorithm introduces some uncertainty in the data.

125

### 126 **3 Quality-based transformation of 3D polar data into 2D Cartesian data**

127

128 The raw data volume is organised in a set of scans consisting of measurement gates expressed  
129 in polar coordinates: scan elevation angle ( $\varepsilon$ ), azimuth ( $\alpha$ ), and the distance from the radar site  
130 to the gate along the radar beam ( $l$ ). For further processing every scan needs to be transformed  
131 into Cartesian coordinates ( $x, y$ ). This is achieved by looping through all the Cartesian pixels  
132 of the 2D output field and finding the corresponding neighbouring polar gates by means of  
133 trigonometric functions (Elo, 2012; Selex, 2010).

134 Here, an algorithm based on spatial interpolation of polar reflectivity data with respect to  
135 quality index  $QI$  data is applied to find the Cartesian reflectivity  $Z$  data as PPI (plan position  
136 indicator) product and generate a corresponding  $QI_{PPI}$  field. Following this, standard products,  
137 such as MAX, VIL, etc., can be generated based on the set of PPIs and related quality  
138 information.

#### 139 **3.1 Generation of quality-based PPI product**

140 PPI is one of the standard Cartesian products that represents reflectivity data generated from a  
141 single radar scan for constant elevation angle  $\varepsilon$ . The algorithm transforms values for  
142 measurement gates of polar coordinates ( $\varepsilon, \alpha, l$ ) into values interpolated for Cartesian pixels  
143 defined by coordinates ( $x, y$ ). The values are projected onto 2D plane although they can  
144 originate from different altitudes. Usually, the transformation is performed while considering  
145 two or four of the closest gates, not considering the quality of particular gates.

146 In the proposed technique, the method of the quality-based interpolation depends on the  
147 density of the gates within the given Cartesian pixel. If the number of the gates is larger than  
148 the preset threshold, that occurs close to the radar, then they all are taken into interpolation  
149 (the so called near-field sub-algorithm); otherwise, i.e. for pixels farther away from the radar,  
150 at the most four gates (independently of their distances to the Cartesian pixel centre) are  
151 considered (the far-field sub-algorithm).

152 In order to distinguish between the near-field and far-field pixels a threshold value for  
 153 distance from the radar site ( $D$ ) is determined by the following function of the measurement  
 154 parameters:

$$155 \quad D = \sqrt{\frac{9500\left(\frac{1.3}{d\alpha} + \frac{2.3}{dl} + 1.6dx\right) - 39000}{\pi}} \quad (1)$$

156 where  $d\alpha$  is the step in azimuth ( $^\circ$ ),  $dl$  is the step in distance from the radar site (km), and  $dx$   
 157 is the spatial resolution of Cartesian pixel (km). For instance, for typical data resolution  $d\alpha =$   
 158  $1^\circ$ ,  $dl = 1$  km, and  $dx = 1$  km, the threshold  $D$  equals 57.5 km. The formula was empirically  
 159 determined based on analysis of the number of gates projected onto particular pixels assuming  
 160 different data spatial resolutions.

161  
 162 *The near-field sub-algorithm.* In cases when the distance from the radar site to the given  
 163 Cartesian pixel does not exceed the threshold distance  $D$ , then the number of gates within the  
 164 pixel is determined. If this number is higher than two, the near-field method based on quality  
 165 weighted interpolation is used:

$$166 \quad Z(x, y) = \frac{\sum_{i=1}^n (Z_i QI_i)}{\sum_{i=1}^n QI_i} \quad (2)$$

167 where  $n$  is the number of gates within the investigated area.  
 168 Otherwise, if the number of gates is not higher than two, the far-field sub-algorithm is  
 169 applied.

170  
 171 *The far-field sub-algorithm.* In the far-field area the closest gates are determined in a different  
 172 way. The coordinates of the Cartesian pixel centre are transformed into polar coordinates and  
 173 the four surrounding gates are taken into account. Generally, the reflectivity for the pixel is  
 174 interpolated from the four corner values (Fig. 1), unless some of the corners (one or two) are  
 175 very close to the considered pixel centre – then only the closest gates are taken into  
 176 calculation.

177

178 Reflectivity in a given pixel with centre in  $(x, y)$  is estimated as weighing an average value  
 179  $Z(x, y)$  from selected gates  $Z_i$ , taking account of both distance to the gates and data quality  
 180 information (quality index  $QI_i$ ):

$$181 \quad Z(x, y) = \frac{\sum_{i=1}^n (Z_i W_{Di} QI_i)}{\sum_{i=1}^n (W_{Di} QI_i)} \quad (3)$$

182 where:  $n$  is the number of the closest gates taken into account (1, 2, or 4);  $W_{Di}$  is the weight  
 183 related to the distance of  $i$ -gate to the pixel centre  $(x, y)$  determined by means of one of the  
 184 standard methods: nearest neighbour, uniform weights, inverse distance to the first or second  
 185 power, bilinear method, or Cressman method. Differences in the overall view of 2D products  
 186 generated employing these methods are not very noticeable. However, they can be significant  
 187 for the estimation of precipitation for small river catchments in cases of flash floods.

### 188 **3.2 Characterisation of PPI product quality**

189 Simultaneously to the determination of reflectivity for each Cartesian pixel  $(x, y)$ , the relevant  
 190 quality index  $QI_{PPI}$  is calculated, depending on the sub-algorithm applied to the data  
 191 interpolation:

192 – for the near-field sub-algorithm:

$$193 \quad QI_{PPI}(x, y) = \frac{\sum_{i=1}^n QI_i}{n}, \quad (4)$$

194 – for the far-field sub-algorithm:

$$195 \quad QI_{PPI}(x, y) = \frac{\sum_{i=1}^n (QI_i W_{Di})}{\sum_{i=1}^n W_{Di}} \quad (5)$$

196

197

## 198 **4 Generation of quality-based 2D radar products based on PPI set**

199

200 The described below algorithms (ETOP, MAX, and VIL) employed for 2D Cartesian product  
 201 generation are standard ones (apart from CONVECTION product which is developed by  
 202 IMGW-PIB for its needs). The proposed approach is to apply quality-based PPIs as input

203 instead of standard ones, which allows to obtain quality-based products. Moreover, the output  
204 products are complemented with related quality fields.

#### 205 **4.1. Standard algorithms for 2D radar products generation**

##### 206 *Echo top product (ETOP)*

207 The echo top (ETOP) product represents a Cartesian image of heights of echo (cloud) tops  
208 defining the cloud boundary at a preset level of radar reflectivity  $Z_0$  (in dBZ). The *ETOP* (in  
209 km) is detected in a preset range of heights (between  $h_{min}$  and  $h_{max}$ ) and generally is  
210 determined by interpolation of reflectivity  $Z$  in pixel  $(x, y)$  between the two highest PPIs for  
211 which the reflectivity passes  $Z_0$  value (Fig. 2a).

##### 212 *Maximum of reflectivity product (MAX)*

213 The maximum of reflectivity (MAX) product represents a Cartesian image of the highest  
214 measured value of radar reflectivity  $Z$  (in dBZ) in each vertical column. Generally, the  
215 product generation involves searching PPIs within a preset range of heights (between  $h_{min}$  and  
216  $h_{max}$ ) for the maximal  $Z$  value in the column (Fig. 2b).

##### 217 *Vertically integrated liquid water (VIL) product*

218 The vertically integrated liquid water (VIL) product represents a Cartesian image of the water  
219 content residing in a user-defined layer in the atmosphere (in dBA). The *VIL* is defined by the  
220 formula:

$$221 \quad VIL \text{ (dBA)} = 10 \log_{10} \int_{h_{min}}^{h_{max}} M(h) dh \quad (6)$$

222 where the liquid water content  $M$  (in  $\text{cm}^3 \text{m}^{-3}$ ) is related to radar reflectivity  $Z$  according to so  
223 called  $Z$ - $M$  relationship (Selex, 2010).

224 The integration range depends on values of both the required heights (between  $h_{min}$  and  $h_{max}$ )  
225 and the measurement scope (between  $h_{lowest}$  and  $h_{highest}$  which are determined for the lowest  
226 and highest PPIs, respectively) – the integration is performed from the lower height of the  
227 bottom limits to the lower height of the upper limits (Fig. 2cd).

## 228 **4.2 Detection of convection (CONVECTION) algorithm**

229 The algorithm for the separation of convective precipitation from stratiform background was  
230 developed as the first stage of the SCENE (Storm Cell Evolution and Nowcasting) model of  
231 precipitation nowcasting which forecasts convective and stratiform precipitation in different  
232 ways (Jurczyk et al., 2015). Radar reflectivity data provide one of the most significant pieces  
233 of information in the algorithm and in an elementary version only radar information is  
234 employed (without data from other sources).

235 The dedicated radar product named CONVECTION is a second-order product as it is  
236 generated not from a set of PPIs but from earlier produced ETOP, MAX, and VIL products.  
237 Moreover, the horizontal structure of the radar reflectivity field turned out to also be a useful  
238 factor for distinguishing between convective and stratiform precipitation, therefore the fields  
239 of parameters computed from the analysis of the spatial structure of the MAX and VIL  
240 (Jurczyk et al., 2012) are factors in CONVECTION field determination: exceedance of the  $Z$   
241 background ( $\Delta Z = Z / Z_{\text{mean}}$ ) and exceedance of the  $VIL$  background ( $\Delta VIL = VIL / VIL_{\text{mean}}$ ).  
242 The two parameters are calculated as a ratio of the value in a considered pixel to the average  
243 of the rain pixels within the surrounding background of an 11-km radius (respectively  $Z_{\text{mean}}$   
244 and  $VIL_{\text{mean}}$  values).

245 The algorithm was designed employing a fuzzy logic approach. For both precipitation classes  
246 (convective  $C$  or stratiform  $S$ ) membership functions  $f_{\text{class}}$  (i.e.  $f_C$  or  $f_S$ ) are defined for the five  
247 parameters described above. Then the functions' values are aggregated as weighted sums for  
248 the classes:

$$249 \quad f_{\text{class}} = \sum_x f_{\text{class}}(x) \cdot W_{\text{class}}(x) \quad (7)$$

250 where  $\text{class}$  is the precipitation class ( $C$  or  $S$ );  $x$  is the particular convection parameter;  $f_{\text{class}}(x)$   
251 is the membership function value for  $x$ -parameter;  $W_{\text{class}}(x)$  is the weight of  $x$ -parameter.  
252 Comparison of the weighted sums for the classes decides which category  $C$  or  $S$  a considered  
253 precipitation pixel belongs to.

254

## 255 **4.3 Characterisation of product quality**

256

257 Generally, the quality of the 2D product  $X$  (e.g. ETOP, MAX, and VIL), expressed by quality  
258 index  $QI_X$ , depends on the two factors:

- 259 – the quality of reflectivity data from which a given product was determined,  $QI_{Xsource}$ ,
- 260 – how large a fraction of investigated heights (between  $h_{min}$  and  $h_{max}$ ) was scanned,
- 261  $QI_{Xscope}$ .

262 The value of the first component  $QI_{Xsource}$  is based on the quality of the PPI products ( $QI_{PPI}$   
 263 from Formulas 4 and 5) defining the given product. Namely:

- 264 –  $QI_{ETOPsource}$  for ETOP is obtained from the  $QI_{PPI}$  value in the pixel for which the *ETOP*  
 265 was observed; and in cases of interpolation from two measurements, the minimum  
 266 quality is chosen,
- 267 –  $QI_{MAXsource}$  for MAX equals the  $QI_{PPI}$  of the pixel for which *MAX* value was observed,
- 268 –  $QI_{VILsource}$  for VIL is an average quality of all PPIs defining the specific *VIL*.

269 For all the products, if the value of a given product equals “nodata”, then the  $QI_{Xsource} =$   
 270 “nodata” (and also the final  $QI_X =$  “nodata”), and if it equals “undetected” then the  $QI_{Xsource} = 1$ .

271 The second component,  $QI_{Xscope}$ , is determined based on the heights of the highest and lowest  
 272 scans for considered Cartesian pixel ( $h_{highest}$  and  $h_{lowest}$  respectively) in relation to  $h_{min}$  and  
 273  $h_{max}$ . Its value depends on what part of the height range between  $h_{min}$  and  $h_{max}$  defining the  
 274 given product was scanned over the given pixel (Fig. 3 and Table 2).

275 The final quality index  $QI_X$  is taken as product of the two components:

$$276 \quad QI_X = QI_{Xsource} \cdot QI_{Xscope} \quad (8)$$

277 The above procedure of quality determination is applied to first-order products like ETOP,  
 278 MAX, and VIL. The quality index for a CONVECTION product is defined by the values of  
 279 the two considered membership functions (see Equation 7):

$$280 \quad QI_{CONVECTION} = \sqrt{\frac{|f_c - f_s|}{f_c + f_s}} \quad (9)$$

281

282

## 283 **5 Validation**

284

285 The effectiveness of quality-based generation of 2D radar products can be indirectly evaluated  
 286 by analysis of statistical properties of investigated product accumulated for longer time  
 287 period, at least one month for the whole radar range (up to 250 km). It is assumed that data

288 reliability can be assessed by symmetry and smoothness (Joe, 2011) expressed in the  
 289 following way:

290 – symmetry coefficient, which is quantified from differences between values  $x$  in pixels  
 291 symmetrical with respect to the centre of the image:

$$292 \quad \text{symmetry} = \frac{\sum_{i=0}^{n-1} x_i}{\text{trunc}(n/2-1) \sum_{i=0}^{\text{trunc}(n/2-1)} |x_i - x_{n-1-i}|} \quad (10)$$

293 where  $i$  is the radar pixel number,  $i \in (0, \dots, n - 1)$ ;  $n$  is the number of pixels in the  
 294 whole radar image;  $\text{trunc}()$  means truncation to integer;

295 – smoothness coefficient, which is evaluated employing a quantity called  $ENL_i$   
 296 (equivalent number of looks) calculated locally around  $i$ -pixel as ratio of squared mean  
 297 and variance within a certain vicinity from the formula:

$$298 \quad ENL_i = \frac{\mu_i^2(X)}{\text{var}_i(X)} \quad (11)$$

299 where  $\mu_i$  is the mean value in 5-pixel vicinity (grid of  $11 \times 11 = 121$  pixels) of  $i$ -pixel;  
 300  $\text{var}_i$  is the variation in the same vicinity. The smoothness is a mean of  $ENL_i$  for the  
 301 whole radar image:

$$302 \quad \text{smoothness} = \frac{1}{n} \sum_{i=0}^{n-1} ENL_i \quad (12)$$

303 The evaluation has been performed for Brzuchania radar on data collected during May and  
 304 June 2014. This radar was selected due to its specific features: location near mountainous area  
 305 and strong presence of spike type echoes from interfering signals (mainly from wi-fi). For this  
 306 reason the quality index field is strongly changeable in space so employing the proposed  
 307 quality-based definition of 2D products can ensure meaningful benefits. The analysis was  
 308 conducted on MAX products generated in a standard way, i.e. from PPIs obtained without  
 309 quality information, and from quality-based PPIs (as described in Sects. 3 and 4).

310 The results of the analysis on two-month accumulations are presented in Table 3. The slightly  
 311 higher values of the both coefficients indicate enhanced reliability of the quality-based MAX  
 312 product in comparison with the standard one.

313 Evaluation of benefits from the proposed quality-based algorithm is difficult because its  
 314 significant impact is observed only on relatively small excerpts of radar images. This impact  
 315 is limited to these places where quality index considerably changes within small distance.  
 316 However, the quality-based products can serve as more reliable input data to rainfall-runoff

317 models in the cases of flash floods and to other applications when very high spatial resolution  
318 is crucial, especially if software is able to take advantage of associated quality field.

319

320

## 321 **6 Example**

322

323 For case study data derived by Brzuchania radar on 27 May 2014 were employed. On that day  
324 convective rainfall with a large number of individual cells and multicell systems was  
325 observed. In Figure 4 a quality index for the lowest scan ( $0.5^\circ$ ) depicted in polar coordinates  
326 is presented together with the raw and corrected reflectivity data.

327 In this case numerous errors were detected, especially the non-meteorological echoes near the  
328 radar site, the external signal interferences (narrow echoes along radar beams), blockage on  
329 terrain in south-west section are the most evident in Figure 4a. A quality index is reduced for  
330 gates where these errors were detected, moreover influence of radar beam broadening (the  $QI$   
331 decreases with distance to the radar) and attenuation in rain (especially in azimuths about  
332  $315^\circ$ ) are noticeable (Fig. 4c). In such a situation the quality index field has a very diversified  
333 spatial pattern and is dynamic in time.

334 The radar data volume, consisting of reflectivity and  $QI$  data, is the basis for the generation of  
335 the 2D products described above. In Figure 5, the products generated from the example  
336 volume are demonstrated: the lowest PPI, ETOP, MAX, VIL, and CONVECTION, along  
337 with the related quality fields.

338 The first four products are similar to ones obtained not taking quality into account because the  
339 changes are evident only locally where  $QI$  values strongly vary from gate to gate. The  
340 relevant quality index fields are mostly influenced by the following factors: distance to the  
341 radar site, presence of wi-fi signals, blockage on terrain, and the fraction of scanned heights  
342 resulting from the scan strategy. The CONVECTION field indicates pixels where convection  
343 is detected according to the algorithm described in Section 4.2. Generally, locations of the  
344 convective areas detected by the algorithm correspond with high values of all three input  
345 products, but pattern of related quality field is more complex. The quality of this product  
346 depends on values of membership functions of both classes and may be connected with the  
347 probability of the presence of convection in a given pixel.

348

## 349 **7 Conclusions**

350

351 Reliable quality information is crucial for user-expected radar-based products because it can  
352 be helpful in the generation of more advanced information for various applications. The  
353 quality index (*QI*) was found to be an appropriate quality metric. A starting point for this  
354 research was processing by means of RADVOL-QC software, which corrects 3D weather  
355 radar data and provides the total *QI* for each gate as a result of considering selected quality  
356 factors.

357 The proposal to generate some 2D products from 3D raw radar data in a more advanced way,  
358 when compared with standard procedures (e.g. Selex, 2010) is presented here. The main idea  
359 of the proposal is that interpolation of 3D data into a set of PPIs and then into other 2D  
360 products is performed in an optimal way, employing quality information related to each  
361 measurement gate. Here the following quality-based versions of standard products are  
362 defined: Echo Top, MAX, and VIL. Moreover, the CONVECTION product for the  
363 identification of convective precipitation based on the abovementioned products is described  
364 as an example of more advanced quality-based radar products. It is expected that the final  
365 products will be of higher reliability not only thanks to previous correction steps, but also  
366 because of the skilled introduction of quality information into the algorithms of product  
367 generation. Verification on the two-month dataset confirmed a slight improvement. However,  
368 due to employed methodology the validation was performed on the whole radar range  
369 whereas considerable enhancements are limited to smaller areas because of specific pattern of  
370 radar quality field.

371 The quality information assigned to the generated product also seems very important. It is  
372 obvious that individual schemes of quality characterisation for each specific product should  
373 be developed. However, a consistent framework needs to be agreed and implemented. The  
374 paper presents a proposal of such a framework.

375 The essential role of quality information in radar data processing is commonly appreciated.  
376 Areas where it may play an important role include the estimation of radar-based and multi-  
377 source (combined) surface rainfall rate, the generation of more reliable hazard indices for  
378 various services like civil protection or air traffic control, and especially the generation of  
379 probabilistic rainfall fields in the form of data ensemble or percentiles, as well as various  
380 other areas.

381

## 382 **Acknowledgment**

383

384 The paper was prepared within the framework of the BALTRAD and BALTRAD+ Projects  
385 (under the Baltic Sea Region Programme 2007-2013 fund). The authors are especially  
386 grateful to Daniel Michelson (SMHI) and Jarmo Koistinen (FMI) for their cooperation and  
387 inspiring discussions during work on the projects.

388

## 389 **References**

390

391 Einfalt, T. and Michaelides, S.: Quality control of precipitation data. In: Precipitation:  
392 Advances in measurement, estimation and prediction, (Ed. S. Michaelides). Springer-Verlag:  
393 Berlin–Heidelberg, 101–126, 2008.

394 Einfalt, T., Szturc, J., and Ośródk, K.: The quality index for radar precipitation data: a tower  
395 of Babel? Atmos. Sci. Let., 11, 139–144, 2010.

396 Elo, C. A.: Correcting and quantifying radar data. Met.no report, 2/2012, pp. 34, 2012.

397 Fornasiero, A., Alberoni, P.P., Amorati, R., Ferraris, L., and Taramasso, A.C.: Effects of  
398 propagation conditions on radar beam-ground interaction: impact on data quality. Advances in  
399 Geoscience, 2, 201–208, 2005

400 Germann, U. and Joss, J.: Operational measurement of precipitation in mountainous terrain.  
401 In: Weather Radar: Principles and advanced applications, (Ed. P. Meischner). Springer-  
402 Verlag, Berlin – Heidelberg, 52–77, 2004.

403 Germann, U., Berenguer, M., Sempere-Torres, D., and Zappa, M.: REAL – ensemble radar  
404 precipitation estimation for hydrology in a mountainous region. Quarterly Journal of Royal  
405 Meteorological Society, 135, 445–456, 2009.

406 Gonzalez-Ramirez, E. and Cluckie, I.D.: Polar to Cartesian coordinate conversion algorithm  
407 and its effects over radar rainfall estimation. ENINVIE, Zacatecas, Zac, 1-6, 2006.

408 Harrison, D.L., Scovell, R.W., and Kitchen, M.: High resolution precipitation estimates for  
409 hydrological uses. Proc. ICE: Water Management, 162, 125-135, 2009.

410 Heistermann, M., Jacobi, S., and Pfaff, T.: An open source library for processing weather  
411 radar data (*wradlib*). Hydrol. Earth Syst. Sci., 17, 863–871, 2013.

412 Henja, A. and Michelson, D.: Improved polar to Cartesian radar data transformation. Proc.  
413 29th AMS Conf. on Radar Meteorology, Montreal, 252-255, 1999.

414 Joe, P.: The WMO radar QC QPE inter-comparison Project RQQL. WMO/CIMO/IOC-RQQL  
415 dokument, 2011 ([www.wmo.int/pages/prog/www/IMOP/meetings/RS/IOC-RQQL-](http://www.wmo.int/pages/prog/www/IMOP/meetings/RS/IOC-RQQL-1/Doc.2.pdf)  
416 [1/Doc.2.pdf](http://www.wmo.int/pages/prog/www/IMOP/meetings/RS/IOC-RQQL-1/Doc.2.pdf)).

417 Jurczyk, A., Ośródk, K., and Szturc, J.: Convective cell identification using multi-source  
418 data. IAHS Publ., 351, 360–365, 2012.

419 Jurczyk, A., Szturc, J., and Ośródk, K.: SCENE: nowcasting for convective and stratiform  
420 precipitation. (In preparation), 2015.

421 Michelson, D., Einfalt, T., Holleman, I., Gjertsen, U., Friedrich, K., Haase, G., Lindskog, M.,  
422 and Jurczyk, A.: Weather radar data quality in Europe: Quality control and characterisation.  
423 Review. COST Action 717 – Use of radar observations in hydrological and NWP models,  
424 Luxembourg 2005, pp. 87, 2005.

425 Michelson, D., Koistinen, J., Peltonen, T., Szturc, J., and Rasmussen, M.R.: Advanced  
426 weather radar networking with BALTRAD+. Proc. 7<sup>th</sup> European Conference on Radar in  
427 Meteorology and Hydrology ERAD 2012, Toulouse, France (CD), 2012.

428 Michelson, D.B., Lewandowski, R., Szewczykowski, M., Beekhuis, H., and Haase, G.:  
429 EUMETNET OPERA weather radar information model for implementation with the HDF5  
430 file format. Version 2.2. EUMETNET OPERA Document, 2014.

431 Norman, K., Gaussiat, N., Harrison, D., Scovell, R., and Boscacci, M.: A quality index for  
432 radar data. EUMETNET OPERA Document, 2010.

433 Ośródk, K., Jurczyk, A., Dziewit, Z., Szturc, J., and Korpus, L.: MeteoFlight: System of  
434 weather hazard monitoring for air traffic control. Proc. 6<sup>th</sup> European Conference on Radar in  
435 Meteorology and Hydrology ERAD 2010, Sibiu, Romania (CD), 2010.

436 Ośródk, K., Szturc, J., and Jurczyk, A.: Chain of data quality algorithms for 3-D single-  
437 polarization radar reflectivity (RADVOL-QC system). Meteorol. Appl., 21, 256–270, 2014.

438 Selex: Rainbow 5. Products and algorithms. Release 5.31.0. Selex SI GmbH, Neuss, pp. 442,  
439 2010.

440 Szturc, J., Michelson, D., Koistinen, J., Haase, G., Peura, M., Gill, R., Sørensen, M., Ośródk,  
441 K., and Jurczyk, A.: Data quality in the BALTRAD+ project. Proc. 7th European Conference  
442 on Radar in Meteorology and Hydrology ERAD 2012, Toulouse, France (CD), 2012a.

443 Szturc, J., Ośródk, K., and Jurczyk, A.: Quality control algorithms applied on weather radar  
444 reflectivity data. In: Doppler radar observations – weather radar, wind profiler, ionospheric  
445 radar, and other advanced applications, (Eds. J. Bech and J. L. Chau). InTech, 289–306,  
446 2012b.

447 Villarini, G. and Krajewski, W.F.: Review of the different sources of uncertainty in single  
448 polarization radar-based estimates of rainfall. *Surv. Geophys.*, 31, 107–129, 2010.

449 Table 1. Scan parameters currently used in the POLRAD weather radar network of IMGW-  
450 PIB.

451

<b>Parameter</b>	<b>Value</b>
Radar beam width	1°
Number of azimuths	360
Maximum range from radar site	250 km
Distance between sampling along radar beam	1 km
Number of elevations	10
Elevation angles (°)	0.5, 1.4, 2.4, 3.4, 5.3, 7.7, 10.6, 14.1, 18.5, 23.8

452

453 Table 2. Scheme of algorithm for  $QI_{Xscope}$  determination.

454

Case	$QI_{Xscope}$ determination
$h_{highest} \leq h_{min}$	$QI_{Xscope} = \text{"nodata"}$ (and $QI_X = \text{"nodata"}$ )
$h_{min} \leq h_{highest} \leq h_{max}$ and $h_{lowest} \leq h_{min}$	$QI_{Xscope} = \frac{h_{highest} - h_{min}}{h_{max} - h_{min}}$
$h_{highest} \geq h_{max}$ and $h_{lowest} \leq h_{min}$	$QI_{Xscope} = 1$
$h_{highest} \geq h_{max}$ and $h_{min} \leq h_{lowest} \leq h_{max}$	$QI_{Xscope} = \frac{h_{max} - h_{lowest}}{h_{max} - h_{min}}$  but for ETOP if $ETOP \neq \text{undetected}$  then $QI_{ETOPscope} = 1$
$h_{lowest} \geq h_{max}$	$QI_{Xscope} = \text{"nodata"}$ (and $QI_X = \text{"nodata"}$ )

455

456 Table 3. Criteria of reliability of standard and quality-based MAX products (Brzuchania  
457 radar, May-June 2014).

458

<b>Criterion</b>	<b>Standard MAX</b>	<b>Quality-based MAX</b>
<i>symmetry</i>	1.582	1.588
<i>smoothness</i>	92.44	92.83

459

460 **Figures**

461

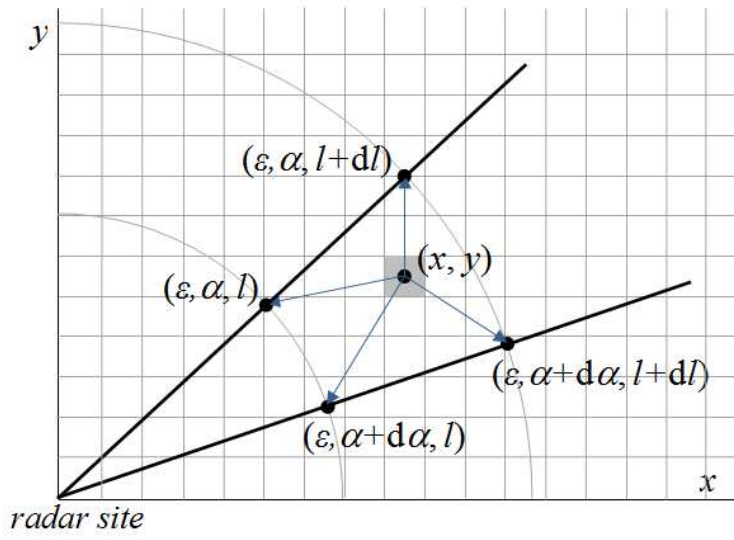
462 Fig. 1. Scheme of interpolation of gate values into Cartesian pixel.

463 Fig. 2. Schemes of generation of products from reflectivity Z values at particular PPIs: (a)  
464 Echo Top, ETOP; (b) maximum of reflectivity, MAX; (c and d) vertically integrated liquid  
465 water, VIL (cases for the highest measurement gate above and below the highest  
466 measurement level).

467 Fig. 3. Quality  $QI_{Xscope}$  determination for 2D product in terms of fraction of scanned heights.

468 Fig. 4. The lowest scan ( $0.5^\circ$ ) in volume from Brzuchania radar, 27 May 2014, 1430 UTC, in  
469 polar coordinates: (a) raw data, (b) corrected data, (c) quality index.

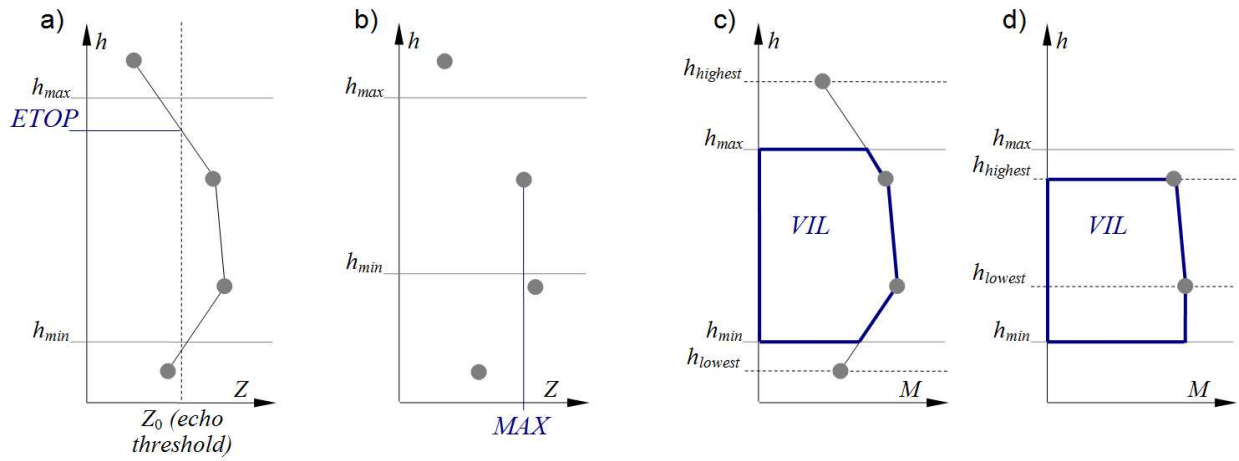
470 Fig. 5. Cartesian radar products with their quality fields: (a) PPI at  $0.5^\circ$ , (b) ETOP with 4 dBZ  
471 as cloud boundary, (c) MAX, (d) VIL, (e) CONVECTION (Brzuchania radar, 27 May 2014,  
472 1430 UTC, distance up to 250 km).



473

474

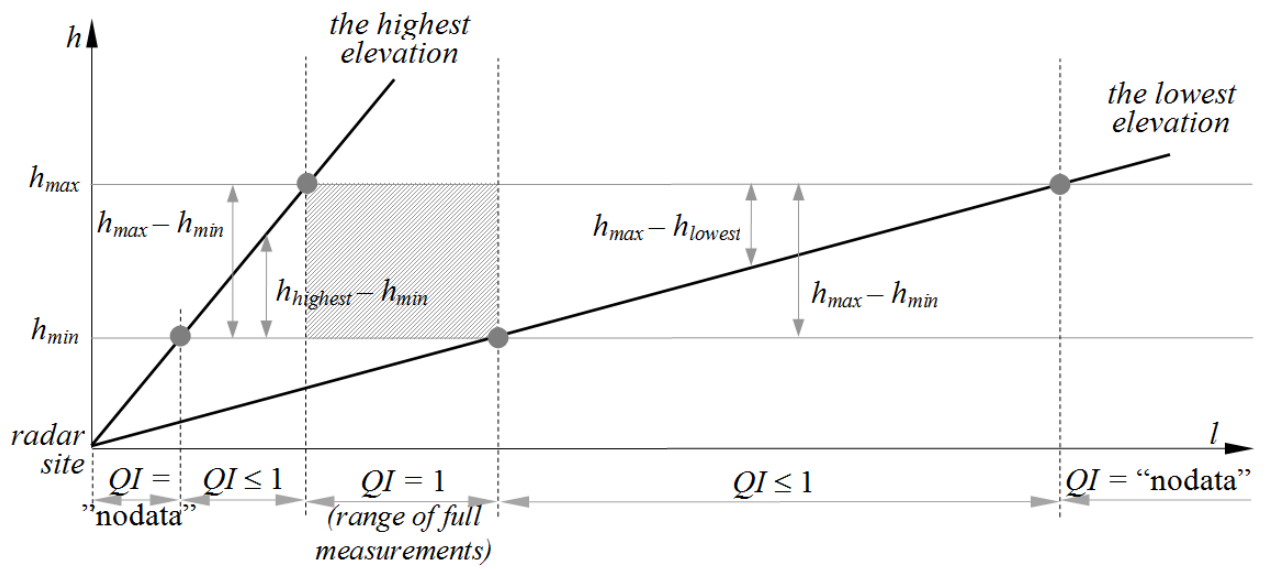
475 Fig. 1. Scheme of interpolation of gate values into Cartesian pixel.



476

477

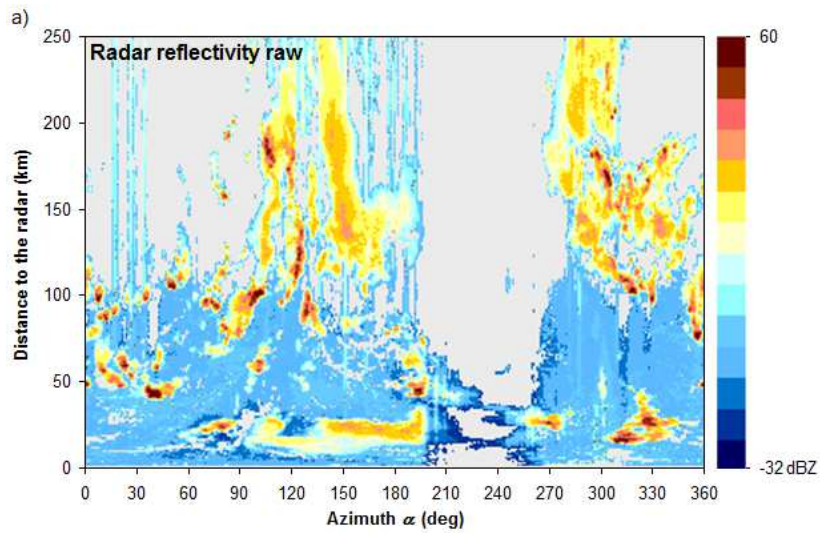
478 Fig. 2. Schemes of generation of products from reflectivity  $Z$  values at particular PPIs: (a)  
 479 Echo Top, ETOP; (b) maximum of reflectivity, MAX; (c and d) vertically integrated liquid  
 480 water, VIL (cases for the highest measurement gate above and below the highest  
 481 measurement level).



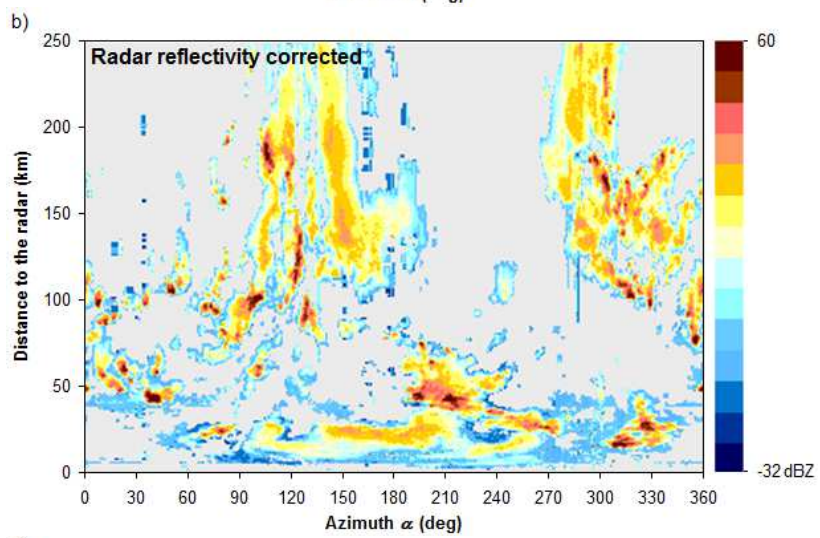
482

483

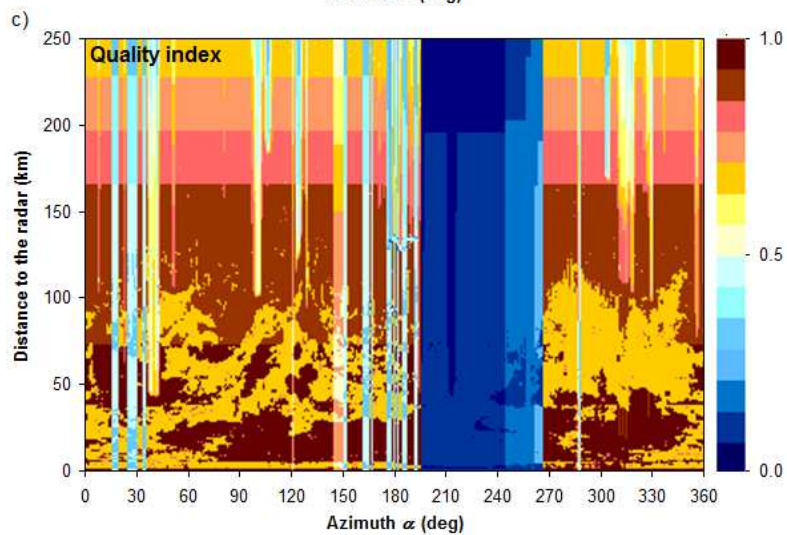
484 Fig. 3. Quality  $QI_{Xscope}$  determination for 2D product in terms of fraction of scanned heights.



485



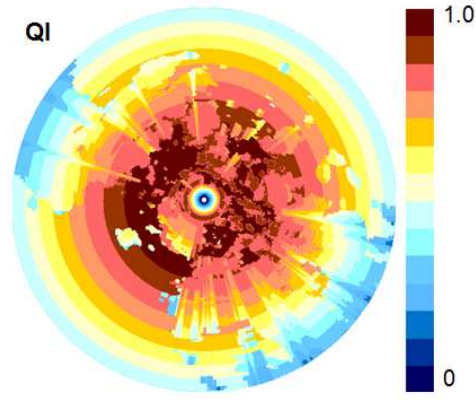
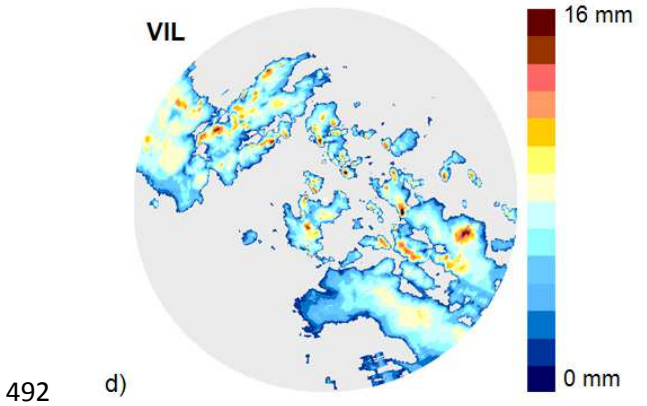
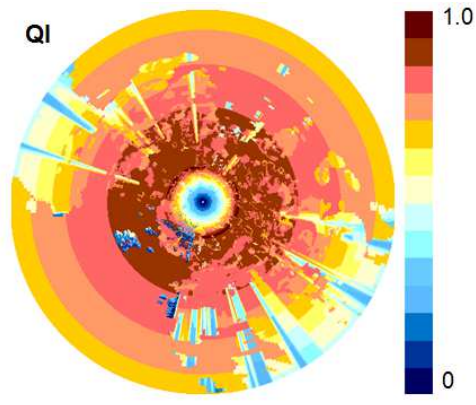
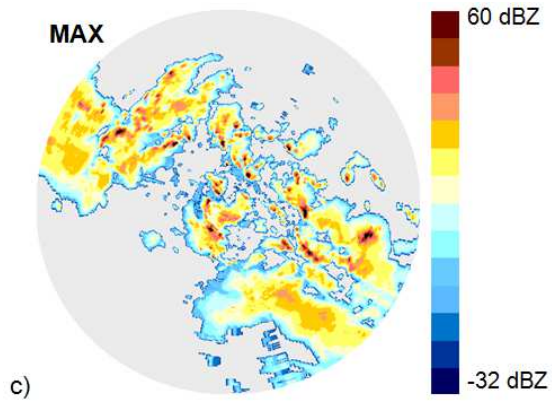
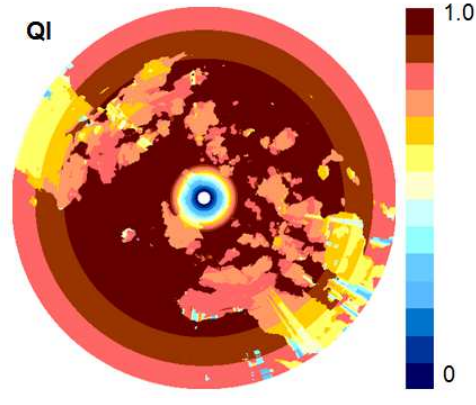
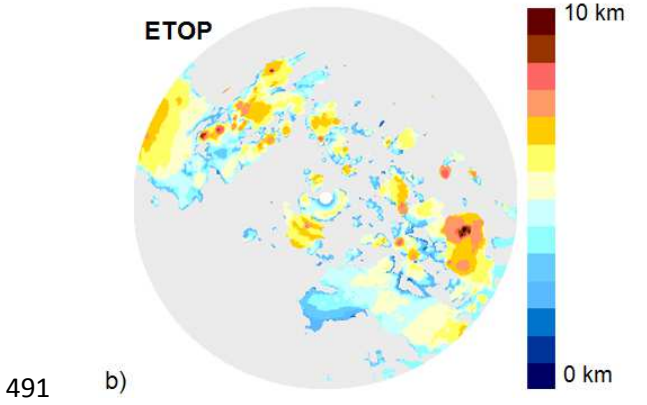
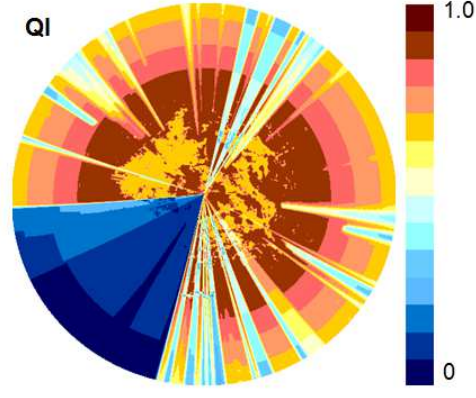
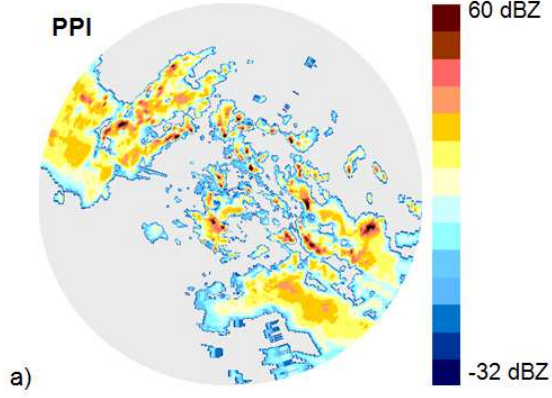
486

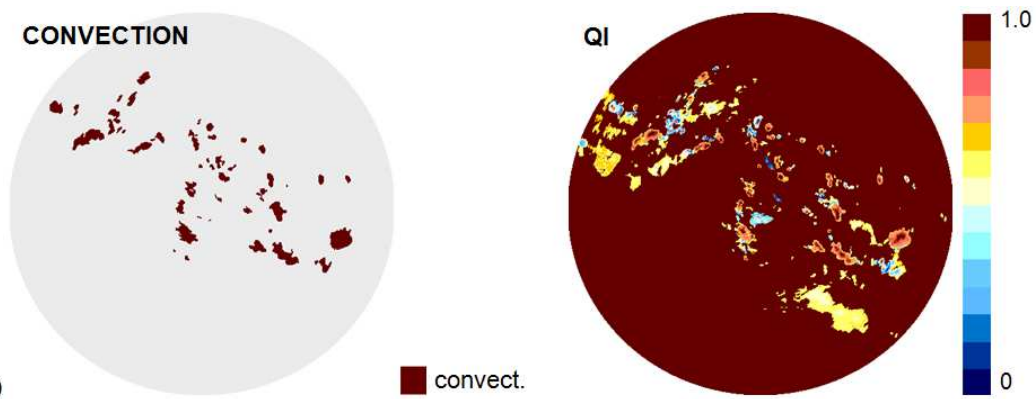


487

488

489 Fig. 5. The lowest scan ( $0.5^\circ$ ) in volume from Brzuchania radar, 27 May 2014, 1430 UTC, in  
 490 polar coordinates: (a) raw data, (b) corrected data, (c) quality index.





493 e)

494

495 Fig. 5. Cartesian radar products with their quality fields: (a) PPI at 0.5°, (b) ETOP with 4 dBZ  
 496 as cloud boundary, (c) MAX, (d) VIL, (e) CONVECTION (Brzuchania radar, 27 May 2014,  
 497 1430 UTC, distance up to 250 km).

498